ISSN 1674-1056
http://cpb.iphy.ac.cn
http://iopscience.iop.org/cpb
中国物理 B
Chinese Physics
中国物理 Chinese Physics B

Simulation of a-Si: H/c-Si heterojunction solar cells: From planar junction to local junction

Haibin Huang(黄海宾)[1], Lang Zhou(周浪)[1], Jiren Yuan(袁吉仁)[1,2], Zhijue Quan(全知觉)[3]
Citation: Chin. Phys. B . 2019, 28(12): 128503 . **doi:** 10.1088/1674-1056/ab5212
Journal homepage: http://cpb.iphy.ac.cn; http://iopscience.iop.org/cpb

What follows is a list of articles you may be interested in

Thermal resistance matrix representation of thermal effects and thermal design of microwave power HBTs with two-dimensional array layout

Rui Chen(陈蕊), Dong-Yue Jin(金冬月), Wan-Rong Zhang(张万荣), Li-Fan Wang(王利凡), Bin Guo(郭斌), Hu Chen(陈虎), Ling-Han Yin(殷凌寒), Xiao-Xue Jia(贾晓雪)
Chin. Phys. B . 2019, 28(9): 098502 . **doi:** 10.1088/1674-1056/ab3436

Improving robustness of GGNMOS with P-base layer for electrostatic discharge protection in 0.5-μm BCD process

Fei Hou(侯飞), Ruibo Chen(陈瑞博), Feibo Du(杜飞波), Jizhi Liu(刘继芝), Zhiwei Liu(刘志伟), Juin J Liou(刘俊杰)
Chin. Phys. B . 2019, 28(8): 088501 . **doi:** 10.1088/1674-1056/28/8/088501

Effect of defects properties on InP-based high electron mobility transistors

Shu-Xiang Sun(孙树祥), Ming-Ming Chang(常明铭), Meng-Ke Li(李梦珂), Liu-Hong Ma(马刘红), Ying-Hui Zhong(钟英辉), Yu-Xiao Li(李玉晓), Peng Ding(丁芃), Zhi Jin(金智), Zhi-Chao Wei(魏志超)
Chin. Phys. B . 2019, 28(7): 078501 . **doi:** 10.1088/1674-1056/28/7/078501

Dark count rate and band to band tunneling optimization for single photon avalanche diode topologies

Taha Haddadifam, Mohammad Azim Karami
Chin. Phys. B . 2019, 28(6): 068502 . **doi:** 10.1088/1674-1056/28/6/068502

Simulation and experimental study of a novel bifacial structure of silicon heterojunction solar cell for high efficiency and low cost

Haibin Huang(黄海宾), Gangyu Tian(田罡煜), Lang Zhou(周浪), Jiren Yuan(袁吉仁), Wolfgang R. Fahrner, Wenbin Zhang(张闻斌), Xingbing Li(李杏兵), Wenhao Chen(陈文浩), Renzhong Liu(刘仁中)
Chin. Phys. B . 2018, 27(3): 038502 . **doi:** 10.1088/1674-1056/27/3/038502

Simulation of a-Si:H/c-Si heterojunction solar cells: From planar junction to local junction*

Haibin Huang(黄海宾)[1], Lang Zhou(周浪)[1,†], Jiren Yuan(袁吉仁)[1,2,‡], and Zhijue Quan(全知觉)[3]

[1] *Institute of Photovoltaics, Nanchang University, Nanchang* 330031, *China*
[2] *Department of Physics, Nanchang University, Nanchang* 330031, *China*
[3] *National Institute of LED on Si Substrate, Nanchang University, Nanchang* 330096, *China*

(Received 8 September 2019; revised manuscript received 13 October 2019; published online 29 November 2019)

In order to obtain higher conversion efficiency and to reduce production cost for hydrogenated amorphous silicon/crystalline silicon (a-Si:H/c-Si) based heterojunction solar cells, an a-Si:H/c-Si heterojunction with localized p–n structure (HACL) is designed. A numerical simulation is performed with the ATLAS program. The effect of the a-Si:H layer on the performance of the HIT (heterojunction with intrinsic thin film) solar cell is investigated. The performance improvement mechanism for the HACL cell is explored. The potential performance of the HACL solar cell is compared with those of the HIT and HACD (heterojunction of amorphous silicon and crystalline silicon with diffused junction) solar cells. The simulated results indicate that the a-Si:H layer can bring about much absorption loss. The conversion efficiency and the short-circuit current density of the HACL cell can reach 28.18% and 43.06 mA/cm^2, respectively, and are higher than those of the HIT and HACD solar cells. The great improvement are attributed to (1) decrease of optical absorption loss of a-Si:H and (2) decrease of photocarrier recombination for the HACL cell. The double-side local junction is very suitable for the bifacial solar cells. For an HACL cell with n-type or p-type c-Si base, all n-type or p-type c-Si passivating layers are feasible for convenience of the double-side diffusion process. Moreover, the HACL structure can reduce the consumption of rare materials since the transparent conductive oxide (TCO) can be free in this structure. It is concluded that the HACL solar cell is a promising structure for high efficiency and low cost.

Keywords: silicon solar cell, a-Si:H/c-Si heterojunction, short-circuit current, local junction

PACS: 85.30.De, 88.30.gg, 85.60.Gz **DOI:** 10.1088/1674-1056/ab5212

1. Introduction

In the past few decades, hydrogenated amorphous silicon/crystalline silicon (a-Si:H/c-Si) based heterojunction solar cells have been attractive since they possess high open-circuit voltage (V_{oc}), low-cost fabrication process and low temperature coefficient.[1–10] In 1992, Panasonic company developed an a-Si:H/c-Si heterojunction structure called the HIT (heterojunction with intrinsic thin-layer) solar cell.[1] Up to now, the conversion efficiency of the typical HIT solar cell has reached 24.7%.[4] For the HIT solar cell, the doped a-Si:H layer at the illumined front of the cell acts as the emitter, and the intrinsic a-Si:H layer plays a role of passivating defects. However, the a-Si:H material can bring about large optical absorption because it possesses a very high absorption coefficient. Holman *et al.*[11] showed theoretically that a relative efficiency increase of over 5% is possible for the heterojunction solar cell by mitigating parasitic absorption. In order to minimize the absorption loss of the a-Si:H, some researchers attempted to develop high-quality wide-gap alloys, such as a-SiC:H,[12] a-SiO$_x$:H,[13] μc-SiO$_x$:H[14] and μc-3C-SiC,[15] to replace a-Si:H as an emitter of the heterojunction solar cell. However, so far, the performance improvement of the solar cell is limited. The reason may be that the property of alternative materials is not good enough and big band offset deteriorates cell performance.[12,16] Several groups[17–21] reported that the emitter of the a-Si:H layer can be placed at the back side of the cell for avoiding the absorption of the doped a-Si:H layer, i.e., interdigitated back contact (IBC) technology has been used for the silicon heterojunction solar cell. The solar cell with the combination of the HIT and IBC technologies has achieved a world-record efficiency of over 26%.[20,21] However, the structure with the HIT and IBC technologies is very complicated, and it is not convenient to fabricate for mass production. In our previous work,[22] we employed an n-type c-Si layer as the emitter, in other words, the doped and intrinsic a-Si:H layers are replaced by n-type c-Si for reducing the optical absorption loss. This device is called the HACD (heterojunction of amorphous silicon and crystalline silicon with diffused junction) cell. However, the c-Si emitter in this structure, which is heavy doped, can make more recombination since the surface of the silicon wafer is also the region where the photocarriers are most generated. In order to overcome the above issues,

*Project supported by the National Key R&D Program of China (Grant No. 2018YFB1500403), the National Natural Science Foundation of China (Grant Nos. 11964018, 61741404, and 61464007), and the Natural Science Foundation of Jiangxi Province of China (Grant No. 20181BAB202027).

†Corresponding author. E-mail: lzhou@ncu.edu.cn
‡Corresponding author. E-mail: yuanjiren@ncu.edu.cn

© 2019 Chinese Physical Society and IOP Publishing Ltd

we propose a bifacial heterojunction of amorphous/crystalline silicon with localized p–n structure (HACL cell).[23,24] The HACL cell structure can minimize the absorption loss of the a-Si:H and reduce recombination of photocarriers in the emitter. All of p–n junctions are local for the HACL cell. The local p–n-junction can make the cell keep high open-circuit voltage, and also take full advantage of sunlight and reduce photocarrier recombination. In addition, the TCO layer, in which it contains rare and expensive indium, can be free for the HACL cell so that the cost will be reduced.

In this work, we perform a numerical simulation using the ATLAS program.[25] The effect of the doped a-Si:H layer on the performance of the HIT cell is studied. The structure of the HACL solar cell is designed. The performance improvement mechanism for the HACL cell is explored. The potential performances of the HIT, HACD and HACL cells are evaluated. The HACL cell with single-side planar junction and single-side local junction are analyzed. All n-type or p-type c-Si passivating layers for the HACL cells are discussed.

2. Device model and simulation parameters

Figure 1 illustrates the schematic structure of the HIT, HACD and HACL solar cells used in this study. Figure 1(a) shows the typical HIT solar cell structure, and figure 1(b) shows the HACD solar cell structure which can be used to find detailed information in our previous work.[22] For the HACL solar cell structure, the optical absorber can be n-type c-Si or p-type c-Si, and n-type c-Si is adopted in this work as shown in Fig. 1(c). Each side of the optical absorber is constituted by emitter region and passivating region. Figure 1(d) shows the top view of several units of the HACL cell. Each emitter region comprises of doped and intrinsic a-Si:H layers, whose width is set to about 50 μm, and the electrodes cover on the doped a-Si:H layers. Each passivating region includes heavy doped c-Si (a few tens of nanometers) and SiN_x layers, whose width is set to about 1500 μm. Sunlight is incident from the passivating region into cell. The area of the emitter region covers about 3% of the area of the wafer surface, and the rest of the area of the wafer surface is covered by passivating region.

The ATLAS program is used in this study. The simulation method is based on the Poisson equation, and the electron and hole continuity equations,[25]

$$\mathrm{div}(\varepsilon\nabla\psi) = -\rho, \tag{1}$$

where ψ is the electrostatic potential, ε is the local permittivity, and ρ is the local space charge density. Here ρ is the sum of contribution from all mobile and fixed charges, including electrons, holes and ionized impurities.

$$\frac{\partial n}{\partial t} = \frac{1}{q}\mathrm{div}\boldsymbol{J}_\mathrm{n} + G_\mathrm{n} - R_\mathrm{n}, \tag{2}$$

$$\frac{\partial p}{\partial t} = \frac{1}{q}\mathrm{div}\boldsymbol{J}_\mathrm{p} + G_\mathrm{p} - R_\mathrm{p}, \tag{3}$$

where n and p are the electron and hole concentrations, $\boldsymbol{J}_\mathrm{n}$ and $\boldsymbol{J}_\mathrm{p}$ are the electron and hole current densities, G_n and G_p are the generation rates for electrons and holes, R_n and R_p are the recombination rates for electrons and holes, and q is the magnitude of the charge on an electron.

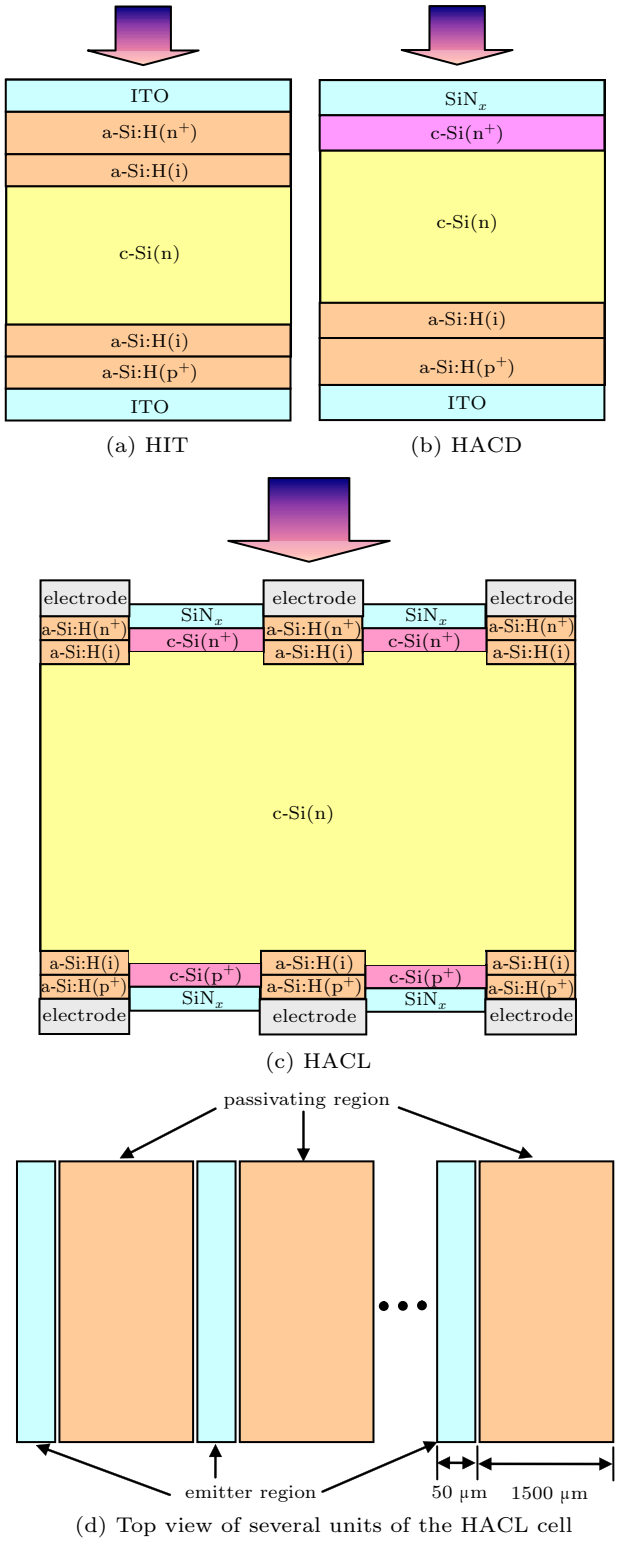


Fig. 1. Schematic of silicon heterojunction solar cells with different structures: (a) HIT, (b) HACD, (c) HACL, and (d) top view of several units of the HACL cell.

For an a-Si:H material, the density of states in the bandgap is assumed to be both acceptor-like states and donor-like states modeled by Gaussian mid-gap states (associated with silicon dangling bonds) and exponential band tails. The conduction and valence band tail states can be described as follows:

$$g_{\mathrm{A}}(E) = G_{\mathrm{AO}} \exp\left(\frac{E - E_{\mathrm{C}}}{E_{\mathrm{A}}}\right), \tag{4}$$

$$g_{\mathrm{D}}(E) = G_{\mathrm{DO}} \exp\left(\frac{E_{\mathrm{V}} - E}{E_{\mathrm{D}}}\right), \tag{5}$$

where $G_{\mathrm{AO}}(E)$ and $G_{\mathrm{DO}}(E)$ are the states per volume per energy for tail states at E_{V} and E_{C}, and E_{A} and E_{D} are the characteristic energies that determine the slopes of their respective tails.

The Gaussian mid-gap states of acceptor-like states and donor-like states are given by

$$g_{\mathrm{A}}(E) = N_{\mathrm{AG}} \left\{ -\frac{1}{2} \left[\frac{(E - E_{\mathrm{AK}})^2}{\sigma_{\mathrm{A}}^2} \right] \right\}, \tag{6}$$

$$g_{\mathrm{D}}(E) = N_{\mathrm{DG}} \left\{ -\frac{1}{2} \left[\frac{(E - E_{\mathrm{DK}})^2}{\sigma_{\mathrm{D}}^2} \right] \right\}, \tag{7}$$

where N_{AG} and N_{DG} are the states per volume per energy for acceptors and donors, E_{AK} and E_{DK} are the peak energy position of Gaussian, and σ_{A} and σ_{D} are the standard deviation of Gaussian acceptors and donors.

The band tail states and Gaussian mid-gap states of doped and intrinsic a-Si:H layers are shown in Fig. 2.

The main material parameters[22,26,27] used in this simulation are listed in Table 1. The simulated condition is under AM 1.5 G, 100 mW/cm^2 and at 300 K.

Table 1. Main parameters used for the simulation of HIT, HACD and HACL solar cells.

Parameters and units	a-Si:H(p$^+$)	a-Si:H(i)	a-Si:H(n$^+$)	c-Si(n)	c-Si(n$^+$/p$^+$) for HACL	c-Si(n$^+$) for HACD
Thickness/nm	10	10	10	1.5×10^5	20	5×10^3
Electron affinity/eV	3.80	3.80	3.80	4.05	4.05	4.05
Band gap/eV	1.72	1.72	1.72	1.12	1.12	1.12
Relative dielectric constant	11.90	11.90	11.90	11.90	11.90	11.90
Effective conduction band density/cm^{-3}	2.50×10^{20}	2.50×10^{20}	2.50×10^{20}	2.80×10^{19}	2.80×10^{19}	2.80×10^{19}
Effective valence band density/cm^{-3}	2.50×10^{20}	2.50×10^{20}	2.50×10^{20}	1.04×10^{19}	1.04×10^{19}	1.04×10^{19}
Electron mobility/cm^2·V^{-1}·s^{-1}	10	20	10	1350	1350	1350
Hole mobility/cm^2·V^{-1}·s^{-1}	2	5	2	450	450	450
Donor concentration/cm^{-3}	0	0	1×10^{19}	3×10^{15}	1×10^{18}	1×10^{18}
Acceptor concentration/cm^{-3}	6×10^{18}	0	0	0	0	0

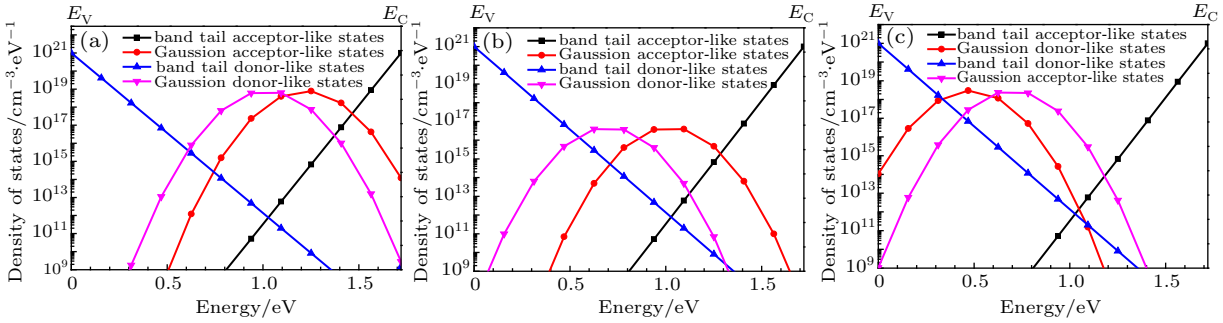


Fig. 2. Gap defect state distribution of (a) a-Si:H(p$^+$), (b) a-Si:H(i), and (c) a-Si:H(n$^+$) layer.

3. Results and discussion

3.1. Effect of the doped a-Si:H layer on the performance of the HIT cells

For an HIT solar cell, the planar junctions are assembled at top and bottom sides of the device. The emitter of the a-Si:H layer entirely covers the surface of the c-Si base. The large absorption coefficient of the a-Si:H material can bring about absorption losses. In order to assess the loss, the performance of the HIT cell is calculated in dependence of variable thicknesses of the top doped a-Si:H layer. Figure 3 shows the photovoltaic parameters of the HIT cells with the emitters of different thicknesses. It is found that the thickness of the doped a-Si:H layer has important impact on the short-circuit current density J_{sc} and efficiency. When the thickness of the doped a-Si:H layer is 2 nm, the J_{sc} and efficiency are 40.21 mA/cm^2 and 25.44%, respectively. If the thickness of the emitter increases to 20 nm, the J_{sc} and efficiency will decrease to 37.32 mA/cm^2 and 23.57%, respectively. The emitter thickness has slight effect on the V_{oc} and fill fact (FF). In order to further clarify the absorption losses, the internal quantum efficiency (IQE) curves are plotted for the HIT cells with the emitters of different thicknesses. It is seen from Fig. 4 that the a-Si:H layer mainly reduces short-wavelength quantum ef-

ficiency, and the cell IQE in the waveband of 300–600 nm decreases with increasing the thickness of the doped a-Si:H layer. Of course, the intrinsic a-Si:H layer will also make absorption loss, but its absorption loss is less than that made by the doped a-Si:H since the doped a-Si:H has more defects. These results indicate that the a-Si:H material can result in the IQE deterioration and thus J_{sc} loss.

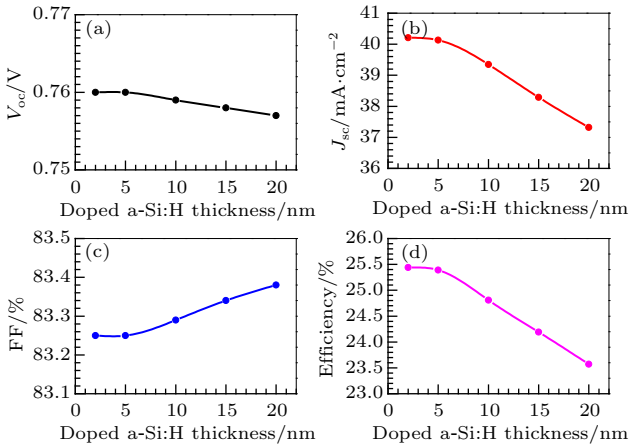


Fig. 3. Photovoltaic parameters of the HIT cells with the emitters of different thicknesses.

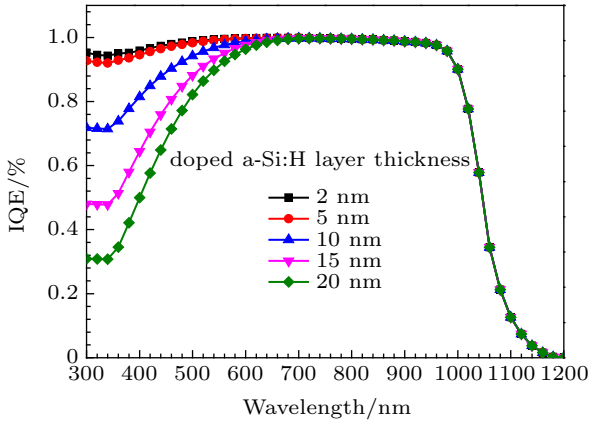


Fig. 4. IQE curves of the HIT cells with the emitters of different thicknesses.

3.2. Performance improvement mechanism for HACL cells

In order to minimize the absorption loss of a-Si:H, the local p–n junctions are designed for the HACL cells. The photogeneration rate and the recombination rate are calculated as shown in Fig. 5. Figures 5(a) and 5(c) show the photogeneration rate and the recombination rate made in the region that is perpendicular to the emitter region surface (assuming that the electrode is transparent). Figures 5(b) and 5(d) show the ones made in the region that is perpendicular to the passivating region surface. It is observed that the photogeneration rate in the a-Si:H layer is greater than that in the c-Si layer. The reason is that the optical absorption coefficient of a-Si:H is larger than that of c-Si. However, most of the photocarriers generated in a-Si:H cannot be attributed to photocurrent since the a-Si:H material possesses high defect density and very low mobility. It can be seen from Figs. 5(c) and 5(d) that the recombination rate in the a-Si:H layer is 2–3 orders of magnitude larger than that in the c-Si layer. Thus, fewer area of of a-Si:H layer that used for the emitter should be favorable. In the HACL cell, the area of the a-Si:H layer just accounts for about 3% of the surface of the c-Si base. It can significantly reduce the absorption loss of a-Si:H so that more photons can be entered into the cell absorber to generate photocarriers. This is demonstrated by Figs. 3 and 4. Noted that a-Si:H acting as the emitter of local junction can keep high V_{oc} for solar cells.

Compared to the HACD cell, the HACL structure can reduce the photocarrier recombination in the emitter. For the HACL cell, most of the surface area is covered by the c-Si passivating layer. The c-Si passivating layer is very thin (about dozens of nanometers), so the recombination quantity is little. Moreover, the recombination rate in the c-Si passivating layer is not large. We can see from Fig. 5(d) that the recombination rate in the c-Si passivating layer (close to the Si_3N_4 layer) is even less than that in the c-Si base. The role of the c-Si passivating layer is to suppress the carrier recombination via n^+–n high-low junction. As a result, the HACL structure can reduce photocarrier recombination and make a high J_{sc}.

For the HACL cell, its structure can help photocarriers to be better transported and collected. In order to illustrate the argument, the vector of electric field for the top side of the part HACL cell is plotted as shown in Fig. 6. It is observed that the main electric field direction in the emitter region is from n^+-a-Si:H to the i-a-Si:H layer, then to the n-c-Si absorber, and that in the passivating region is from n^+-c-Si to the n-c-Si layer. Thus, a large number of minority carriers (here is hole) generated at the c-Si wafer surface are driven into cell inside, and then they are transported to local p–n junction and collected by electrodes (on the local p–n junction). This process can avoid lateral transport for minority carriers so that it can improve collection efficiency of minority carriers. For traditional planar junction, lateral transport of minority carriers generated at the surface of the c-Si base can result in more recombination since there is heavy doping in the emitter layer. Therefore, the local p–n junction can make high J_{sc} since the collection efficiency of photocarriers can be improved.

To verify the advantage of the HACL structure, potential performances of the HIT, HACD and HACL cells are calculated. Figure 7 shows the simulation results of the potential performances of the HIT, HACD and HACL cells. It is found that the HACL cell has the highest conversion efficiency. If sunlight is incident from the top side of the cell, a conversion efficiency of 27.84% for the HACL cell can be achieved, while for the HACD and HIT cells, their conversion efficiencies

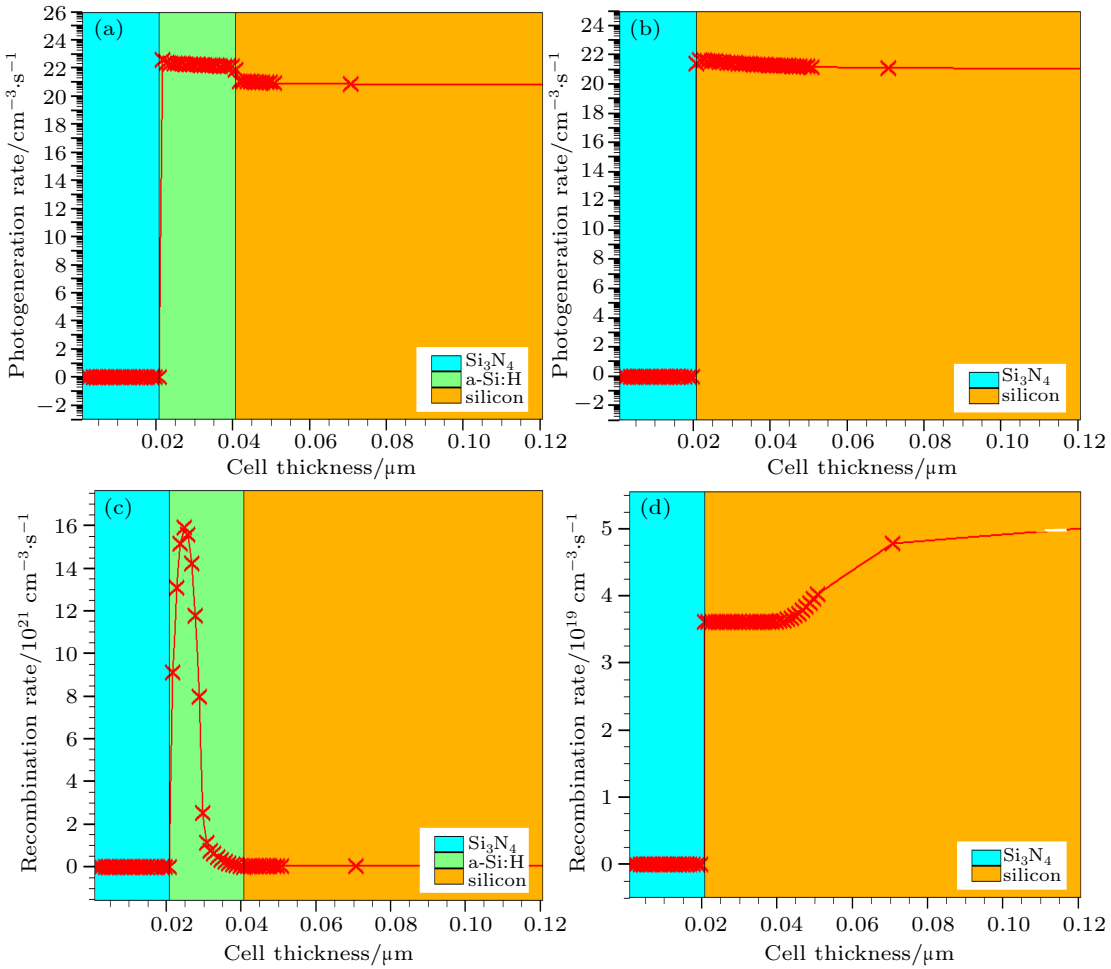


Fig. 5. The photogeneration rate and the recombination rate of different regions for the HACL cell: (a) and (c) for the region that is perpendicular to the emitter region surface, (b) and (d) for the region that is perpendicular to the passivating region surface.

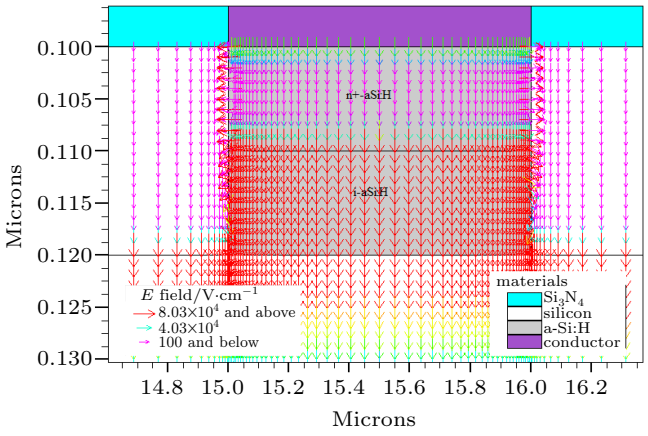


Fig. 6. Vector of electric field for the top side of the part HACL cell.

are 27.35% and 26.58%, respectively. When the illumination enters from bottom side of the cell, the potential conversion efficiencies of the HIT, HACD and HACL cells are 26.53%, 27.03% and 28.18%, respectively. The differences of conversion efficiency of the three cells mainly depend on the short-circuit current density. It can be seen from Fig. 6(a) that the J_{sc} of the HACD cell is higher than that of the HIT cell. This is because a-Si:H layers in the HIT cell can bring about much

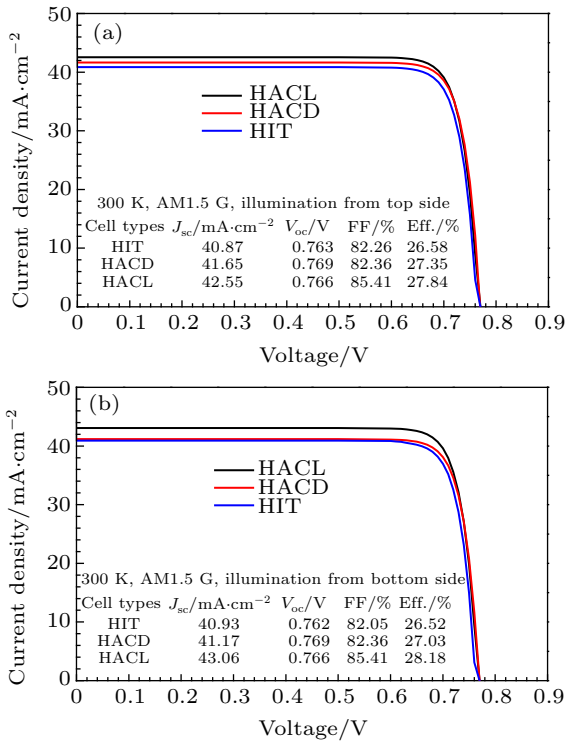


Fig. 7. Potential performances of the HIT, HACD and HACL cells: (a) illumination from top side, (b) illumination from bottom side.

optical absorption loss. For the HACL cell, its high J_{sc} may be attributed to two aspects. One is that the area of the a-Si:H layer is minimized to reduce absorption loss. The other is that the local junction can improve the collection efficiency of photocarriers.

Here it should be noted that in our previous work[22] a conversion efficiency of 28.55% can be achieved for an optimized HAC cell (i.e. the HACD cell in this paper), while the conversion efficiency of the HACL cell can just reach 28.12% in this work. The main reason is that in our previous work we assumed that the light trapping in the cell was idealized and the surface passivation of the wafer was perfect. In this work, in order to obtain more "real" results, the set parameters of surface recombination velocity and surface reflectance for the HACL cell are somewhat strict. Hence, the calculated conversion efficiency of the HACL cell is even slightly lower than that of the HACD cell reported in Ref. [22]. In this work, we set the same parameters about surface recombination velocity and surface reflectance for the HACD and HACL cells. Figure 7 proves that the performance of the HACL cell is better than that of the HACD cell. Moreover, it should be stressed that the production cost of the HACL cell would be markedly reduced since it is a TCO-free structure. We will talk about this point in Section 3.5.

In Table 2, the photovoltaic performances of the recent a-Si:H/c-Si based heterojunction solar cells are compared with that of the HACL solar cell. It is found that the conversion efficiency of the HACL cell is higher than that of the HIT or HIT+IBC cells. Though the conversion efficiency of 28.18% for the HACL cell is a calculated value, its efficiency goal is encouraging. Moreover, there is a cost advantage for the HACL cell.

Table 2. Performance comparison of recent a-Si:H/c-Si based cells with the HACL cell.

Cell type	V_{oc}/V	J_{sc}/mA·cm^{-2}	FF/%	efficiency/%	References	Remark
HIT	0.750	39.50	83.2	24.70	[4]	experimental data
HIT	0.738	40.80	83.5	25.10	[28]	experimental data
HIT + IBC	0.740	41.80	82.7	25.60	[29]	experimental data
HIT + IBC	0.738	42.65	84.9	26.70	[9], [20]	experimental data
HIT	0.769	41.71	84.24	27.02	[30]	simulation results
HIT	0.763	39.28	85.98	25.75	[31]	simulation results
HACL	0.766	43.06	85.41	28.18	This work	simulation results

3.3. HACL cell with single-side planar junction and single-side local junction

In order to further probe the role of the local junction, a planar junction is used to replace the local junction at top or bottom side of the above HACL cell. Thus, one side of the designed HACL cell is planar junction, and the other side of the HACL cell is local junction. If the planar junction is placed at top or bottom side, the cell is named as HACL cell-I or HACL cell-Ⅱ. The current-voltage curves of two kinds of cells are plotted as shown in Fig. 8. It is found that the J_{sc} and conversion efficiency of the HACL cell-Ⅱ are higher than that of the HACL cell-I. This should be attributed to the local junction at top side of the HACL cell-Ⅱ, which can make more photons into cell and reduce photocarrier recombination. For the HACL cell-I, its top side is planar junction, in which the a-Si:H layer and the lateral transport of photocarriers at the cell surface can bring about more recombination. Moreover, it is found that the performance of the HACL cell-Ⅱ is almost same as that of the above HACL cell. This result indicates that the local junction at the bottom of the cell has negligible impact on the cell performance since few photocarriers can be generated at the bottom of the cell. The result agrees with the above analysis about local junction. However, if the designed cell is bifacial (double-side), the advantage of the local junction at the bottom of the cell will be well presented.

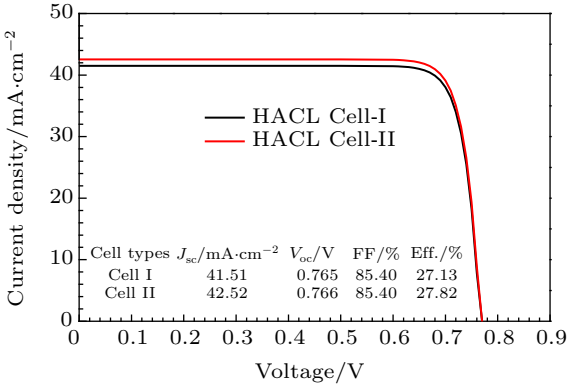


Fig. 8. Current-voltage curves of the HACL cell-I and cell-Ⅱ.

3.4. HACL cell with all n-type c-Si passivating region

It can be seen from Fig. 1(c) that the passivating regions are covered by the n-type (top side) or p-type c-Si layers (bottom side) for the HACL cell. This design will bring about more steps for the production process. If the p-type c-Si passivating layer (bottom side) is replaced by the n-type passivating one, i.e., the passivating layers are all n-type c-Si, it will be convenient to the double-side diffusion process for forming double-side n-type c-Si passivating layers. In order to prove its feasibility, the photovoltaic performances of two kinds of

HACL cells are calculated. The cell with n-type (for top side) and p-type (for bottom side) c-Si passivating layers is named as HACL cell-Ⅲ, and that with all n-type c-Si passivating layers is named as HACL cell-Ⅳ. The calculated results are listed in Table 3. It is found that the photovoltaic performances of the HACL cell-Ⅲ and HACL cell-Ⅳ are very close. Therefore, we can infer that the HACL cell with all n-type c-Si passivating layers can work well. However, it should be noticed that the n-type c-Si passivating region at the bottom must be not connected with i-a-Si:H and p^+-a-Si:H layers in the emitter region. The gap between the passivating region and the emitter region can help to more effectively cut off the lateral transport of photocarriers. Moreover, the lateral p–n junction at the bottom can be avoided to form due to the existence of the gap. In the fabrication process, the gap can be filled by insulator, such as SiN_x.

Similarly, it can be inferred that if the optical absorber of an HACL solar cell is p-type c-Si base, the passivating layers can be all p-type c-Si.

Table 3. Calculated photovoltaic performance of the HACL cell-Ⅲ and cell-Ⅳ.

Cell types	J_{sc}/mA·cm^{-2}	V_{oc}/V	FF/%	Eff/%
Ⅲ	42.55	0.766	85.43	27.84
Ⅳ	42.21	0.766	85.28	27.58

3.5. TCO-free analysis for HACL cells

For the planar junction, a TCO layer must be deposited on the whole a-Si:H layer to effectively collect the current of solar cells since the lateral conductive property of a-Si:H is weak. However, the TCO layer can be free for our HACL cell. The above simulation results prove that the TCO-free HACL cell can obtain high conversion efficiency. The reason may be that the emitter is local, and its width is small. According to our design, the width of the c-Si passivating region is about 1500 μm, and the width of the a-Si:H emitter is about 50 μm. This small emitter width does not affect the collection of current though the lateral conductive property of a-Si:H is weak.

It is well known that TCO materials contain rare and very expensive metals, such as indium. This makes TCO materials account for about 10% of the cost of the entire cell. TCO-free cells also reduce the number of fabrication steps. Therefore, the TCO-free HACL cell can achieve a reduction in production cost. Moreover, the TCO-free cells can reduce the series resistance loss caused by carrier transport in the TCO. Thus, the HACL structure can also improve cell performance and reduce cell cost by the TCO-free way.

4. Conclusions

A numerical simulation has been carried out using the ATLAS program. The effect of the a-Si:H layer on the performance of the HIT cell is studied. The performance improvement mechanism for the HACL cell is explored. The potential performances of the HIT, HACD and HACL cells are evaluated. It is found that the a-Si:H layer can reduce short-wavelength quantum efficiency and decrease short-circuit current density. The HACL cell can reach a conversion efficiency of 28.18% and a short-circuit current density of 43.06 mA/cm^2. The excellent performance for the HACL cell originates from the unique structure design based on local p–n junction. The advantage of the HACL structure is that more photons can be entered into the cell absorber to generate photocarriers since a-Si:H layers are free in the non-junction regions and the collection efficiency of photocarriers can be improved since a very thin passivating layer can reduce photocarrier recombination. The double-side local junction is very suitable for the bifacial solar cells. Furthermore, for an HACL cell with n-type or p-type c-Si base and double-side local junction, all n-type or p-type c-Si passivating layers are feasible for convenience of the double-side diffusion process. Moreover, the TCO materials, in which there is rare and valuable metal element of indium, are free for the HACL structure so that the production cost can be reduced. The results show that the HACL solar cell may be a promising structure for high efficiency and low cost in mass production.

References

[1] Tanaka M, Taguchi M, Matsuyama T, Sawada T, Tsuda S, Nakano S, Hanafusa H and Kuwano Y 1992 *Jpn. J. Appl. Phys.* **31** 3518

[2] Taguchi M, Kawamoto K, Tsuge S, Baba T, Sakata H, Morizane M, Uchihashi K, Nakamura N, Kiyama S and Oota O 2000 *Prog. Photovolt: Res. Appl.* **8** 503

[3] Tsunomura Y, Yoshimine Y, Taguchi M, Baba T, Kinoshita T, Kanno H, Sakata H, Maruyama E and Tanaka M 2009 *Sol. Energy Mater. Sol. Cells* **93** 670

[4] Taguchi M, Yano A, Tohoda S, Matsuyama K, Nakamura Y, Nishiwaki T, Fujita K and Maruyama E 2014 *IEEE J. Photovolt.* **4** 96

[5] Yao Y, Xu X, Zhang X, Zhou H, Gu X and Xiao S 2018 *Mater. Sci. Semicond. Process.* **77** 16

[6] Wu Z, Zhang L, Chen R, Liu W, Li Z, Meng F and Liu Z 2019 *Appl. Surf. Sci.* **475** 504

[7] Zhao L, Wang G, Diao H and Wang W 2018 *J. Phys. D: Appl. Phys.* **51** 045501

[8] Bashiri H, Karami M A and Nejad S M 2017 *Mater. Res. Express* **4** 126308

[9] Green M A, Hishikawa Y, Dunlop E D, Levi D H, Hohl-Ebinger J and Ho-Baillie1 A W Y 2019 *Prog. Photovolt. Res. Appl.* **27** 3

[10] Bashiri H, Karami M A and Mohammadnejad S 2018 *Superlattices Microstruct.* **120** 327

[11] Holman Z C, Descoeudres A, Barraud L, Fernandez F Z, Seif J P, Wolf S D and Ballif C 2012 *IEEE J. Photovolt.* **2** 7

[12] Qiao Z, Ji J, Zhang Y, Liu H and Li T 2017 *Chin. Phys. B* **26** 068802

[13] Ding K, Aeberhard U, Smirnov V, Holländer B, Finger F and Rau U 2013 *Jpn. J. Appl. Phys.* **52** 122304

[14] Banerjee C, Sritharathikhun J, Yamada A and Konagai M 2008 *J. Phys. D: Appl. Phys.* **41** 185107

[15] Ogawa S, Yoshida N, Itoh T and Nonomura S 2007 *Jpn. J. Appl. Phys.* **46** 518

[16] Yang X, Song J, Yang J, Bai J, Dang W and Chen J 2018 *J. Phys. D: Appl. Phys.* **51** 305501

[17] Lu M 2007 *Appl. Phys. Lett.* **91** 063507

[18] Mingirulli N, Haschke J, Gogolin R, Ferre R, Schulze T F, Düsterhöft J, Harder N P , Korte L, Brendel R and Rech B 2011 *Phys. Stat. Solidi-RRL* **5** 159
[19] Lu M, Das U, Bowden S, Hegedus S and Birkmire R 2011 *Prog. Photovol.: Res. Appl.* **19** 326
[20] Yoshikawa K, Kawasaki H, Yoshida W *et al.* 2017 *Nat. Energy* **2** 17032
[21] Yoshikawa K, Yoshida W, Irie T *et al.* 2017 *Sol. Energy Mater. Sol. Cells* **173** 37
[22] Huang H, Tian G, Zhou L, Yuan J, Fahrner W R, Zhang W, Li X, Chen W and Liu R 2018 *Chin. Phys. B* **27** 038502
[23] Huang H, Zhou L, Yuan J, Gao C and Yue Z 2018 Patent CN108336157A, July 27, 2018
[24] Yuan J, Zhou L, Huang H, Gao C and Yue Z 2018 Patent CN108461569A, August 28, 2018
[25] *ATLAS User's Manual—device Simulation Software* 2016 SILVACO Santa Clara CA
[26] Yuan J, Shen H, Lu L, Wu T and He X 2010 *Optoelectron. Adv. Mater.-Rapid Commun.* **4** 1211
[27] Hernandez-Como N and Morales-Acevedo A 2010 *Sol. Energy Mater. Sol. Cells* **94** 62
[28] Adachi D, Hernández J L and Yamamoto K 2015 *Appl. Phys. Lett.* **107** 233506
[29] Masuko K, Shigematsu M, Hashiguchi T *et al.* 2014 *IEEE J. Photovolt* **4** 1433
[30] Dwivedi N, Kumar S, Bisht A, Patel K and Sudhakar S 2013 *Sol. Energy* **88** 31
[31] Yao Y, Xu X, Zhang X, Zhou H, Gu X and Xiao S 2018 *Mater. Sci. Semicond. Process* **77** 16